Water Resources and Industry 12 (2015) 1–7

Contents lists available at ScienceDirect

Water Resources and Industry

journal homepage: www.elsevier.com/locate/wri

Rapid removal of Ni(II) from aqueous solution using 3-Mercaptopropionic acid functionalized bio magnetite nanoparticles

Sada Venkateswarlu, S. Himagirish Kumar, N.V.V. Jyothi *

Analytical & inorganic Division of Chemistry, S.V.University, Tirupati 517502, Andhra Pradesh, India

ARTICLE INFO

Article history:
Received 20 June 2015
Received in revised form
23 August 2015
Accepted 8 September 2015

Keywords:
3 MPA@Fe_3O_4 MNPs
FTIR
TEM
VSM
Ni(II) removal

ABSTRACT

The surfaces of bio magnetite nanoparticles were functionalized with 3-Mercaptopropionic acid (3 MPA) and used as a high-capacity and recyclable adsorbent for the rapid removal of Ni(II) from aqueous solution. The 3 MPA@Fe_3O_4 MNPs were characterized by Fourier transformed infrared analysis (FT-IR), transmission electron microscopy (TEM), energy dispersive X-ray spectroscopy (EDS) and vibrating sample magnetometer (VSM) analysis. This 3 MPA@Fe_3O_4 MNPs have been used for removal of Ni(II) from aqueous solution. The hysteresis loops of 3 MPA@Fe_3O_4 MNPs shows an excellent ferromagnetic behavior with saturation magnetization value of 14.02 emu/g. The adsorption isotherm data were fitted well to Langmuir isotherm, the monolayer adsorption capacity was found to be 42.01 mg/g at 303 K. The experimental kinetic data fitted very well the pseudo-second-order model.The results indicate that the biogenic 3 MPA@Fe_3O_4 MNPs act as significant adsorbent material for removal of Ni(II) aqueous solution and also considered as a potential adsorbent for hazardous metal ions from wastewater.

1. Introduction

In recent years, the toxicity and the effect of heavy metals which are dangerous to public health and environment are attracting more attention from pollution and nutritional fields. Long -term exposures to those dissolved metal ions are consequently affected on the human health and natural ecosystems [1,2]. Industries, including mining, production of stainless steel, paints and batteries, electric boards/circuits manufacturing industries, non-ferrous alloys and electroplating discharge effluents containing high levels of heavy metals such as lead, cadmium, mercury, and nickel [3,4]. Untreated effluents may have an adverse impact on the environment [5,6]. Among this nickel is an important element, the high concentration of nickel causes severe damage to lungs, kidneys, gastrointestinal distress, skin dermatitis, dizziness, cyanosis and chest pain [7–9]. Although nickel is an essential micronutrient for animals and takes part in the synthesis of vitamin B_{12}. But the tolerance limit of nickel in drinking water is 0.01 mg L^{-1}, and for industrial wastewater it is 0.2–2.0 mg L^{-1} [10,11].

To prevent heavy metal pollution, it is important to apply robust and effective purification processes of wastewaters containing elevated concentrations of toxic metals. Several techniques have been employed for the treatment of wastewater containing heavy metal ions including ion flotation [12], reverse osmosis [13], chemical precipitation [14,15], ion exchange [16], electrochemical treatment [17] and solid phase extraction (SPE) [18]. However, these techniques are not economically viable due to higher maintenance, operational costs and time -consuming especially in developing countries. Adsorption technology is presented to be one of the most promising methods to this end [19,20]. Traditional adsorbents such as activated carbon [21,22] low cost natural bio sorbents such as chitosan [23,24] natural inorganic ion exchange materials such as zeolites [25], bentonite [26], moss peat [27] and clay [28–30] suffer from low selectivity, low capacity, and weak binding affinity for heavy metal ions. In addition, separation and recovery of these sorbent materials from the decontaminated water can be extremely challenging. To overcome some of these issues compared to the traditional adsorbent, magnetic adsorbents in nanometer size have attracted great attention for their potential application in removal of the pollutants from aqueous solution due to their strong adsorption capacity, simple recovery by magnetic field and reusable property [31,32]. Owing to magnetic property they are attracted to a magnetic field but do not retain magnetic properties when the field is removed, making them highly useful in novel separation processes [33–35]. Magnetic nanoparticles with or without surface functionalization, have been reported to successfully capture Cd(II) [36] As(II) [37] and Ni(II) [38].

In the present study, we recently synthesized biogenic Fe_3O_4 ferromagnetic nanoparticles [39] used as a new adsorbent to remove Ni(II). The bio magnetite nanoparticles are functionalized with 3-Mercaptopropionic acid (3 MPA). The functionalized 3 MPA@Fe_3O_4 MNPs are characterized by using transmission

* Corresponding author.
E-mail address: nvvjyothi01@gmail.com (N.V.V. Jyothi).

http://dx.doi.org/10.1016/j.wri.2015.09.001

electron microscopy (TEM), energy dispersive X-ray spectroscopy (EDS) and Fourier transformed infrared analysis (FT-IR). 3 MPA@Fe_3O_4 MNPs could achieve high affinity with aqueous Ni (II) and have enhanced adsorption capacity. The optimum adsorption conditions for their removal of Ni(II), adsorption isotherms, and kinetic studies were extensively studied.

2. Experimental section

2.1. Materials and methods

3-mercaptopropanoic acid, $Ni(NO_3)_2 \cdot 6H_2O$, HCl, and NaOH were all purchased from Sigma-Aldrich. Typically, 40 ml of double distilled water was taken in to 100 ml round bottom flask to this 0.926 g of dried biogenic Fe_3O_4 MNPs [39] and 0.424 g 3-mercaptopropanoic acid were mixed to gather by ultrasonication for 10 h at room temperature and pH adjustment was done by adding 0.01 M NaOH solution drop-wise until pH 8 is reached. After 10 h reaction the obtained 3-mercaptopropanoic acid functionalized Fe_3O_4 MNPs were separated by using the external magnetic field, washed with double distilled water and absolute ethanol for triplicates, and finally dried at 95 °C under vacuum.

2.2. Characterization

Jeol JEM-2100 transmission electron microscope (TEM) was used to determine by morphological and size distribution of Fe_3O_4 magnetic nanoparticles, quantitative elemental analysis of the nanoparticles were carried out with Oxford instruments Inca Penta FET $\times 3$ electron diffraction spectrum (EDS). An FTIR measurement was used to determine the vibration frequency changes of the functional groups in the adsorbents being made with Thermo Nicolet FTIR-200 Thermo electron corporation. The magnetization loops for magnetite nanoparticles washed with ethanol were measured at room temperature using a vibrating sample magnetometer (VSM, LKSM- 7410)

2.3. Batch adsorption experiment

The adsorption of Ni(II) ion on to the 3 MPA@Fe_3O_4 MNPs nanocomposite was investigated in aqueous solution by batch adsorption experiments with pH range varied 2–8 at 303 K. Ni(II) stock solution was prepared with different concentrations, and then 2.5 mg of magnetic nano-adsorbent was added to 25 mL of each Ni(II) ion solution. The initial pH of Ni(II) ion was adjusted by using 0.1 M HCl/NaOH solution. The solution mixture was ultrasonication at room temperature for 5 min and transferred to 100 mL Erlenmeyer flask and was shaken in a thermostatic incubator (200 rpm) at 303 K. After that, the magnetic nano-adsorbent was removed magnetically from the solution. The concentration of Ni(II) ions was determine using FAAS (Shimadzu AA-6300). To understand the pH effect (Elico LI 120) the 3 MPA@Fe_3O_4 MNPs dosage was maintained at 0.1 g/L. All the adsorption experiment was repeated triplicate. The adsorption percentage was defined as follows

$$\text{Adsorption}(\%) = \frac{(C_i - C_e)}{C_i} \times 100 \tag{1}$$

The amount of Ni(II) adsorbed by the magnetic nano adsorbent at equilibrium was obtained using the following equation:

$$q_e = \frac{(C_i - C_e)V}{M} \tag{2}$$

where q_e (mg/g) is the equilibrium adsorption capacity of Ni(II). C_i and C_e were initial and equilibrium concentration (mg/L) of Ni (II) respectively, M is the adsorbent dosage (mg), V is the volume of the solution (L).

3. Results and discussion

Magnetic 3 MPA based nanospheres can be used as an adsorbent for Ni(II) removal from aqueous solution and enriched completely within a short time under an external magnetic field as shown in Scheme 1. The combination of magnetic property and absorption performance into one single entity can make the 3 MPA based materials separable magnetically and significantly facilitate their practical applications. The compatibility of this work was that it is relatively simple to handle and environmentally benign as well as very less time consuming due to no further centrifugation required.

3.1. FT-IR studies

FTIR analysis was used for understanding the binding of 3-mercaptopropanoic acid on the surface of Fe_3O_4 and also after adsorption of Ni(II). Fig. 1a shows the 3-mercaptopropanoic acid functionalized Fe_3O_4 MNPs, the bands at 1670, 1480 and 1280 cm^{-1} shows the binding nature of COO^- on the surface of Fe_3O_4 and the band at 3410 cm^{-1} indicates O–H groups present on the surface of Fe_3O_4 MNPs. The bands at 2930 cm^{-1}, 2520 cm^{-1}

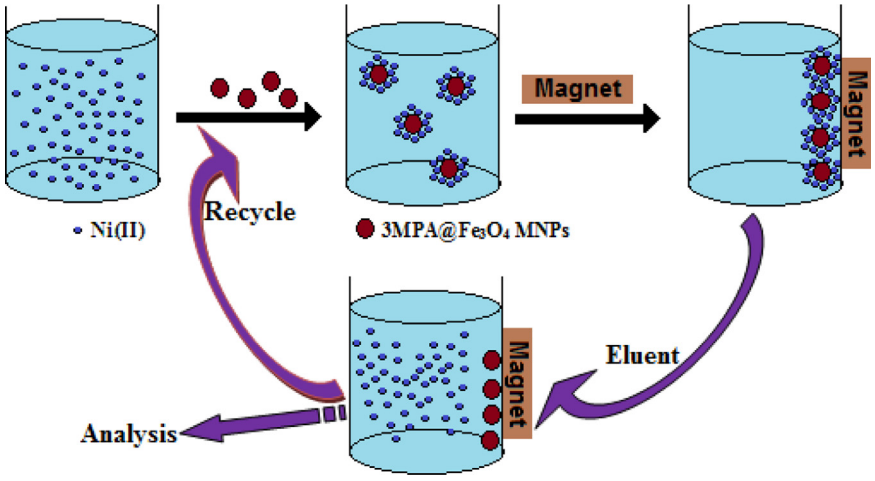

Scheme 1. Ni(II) removal and recycle performance by the aid of an external magnetic field.

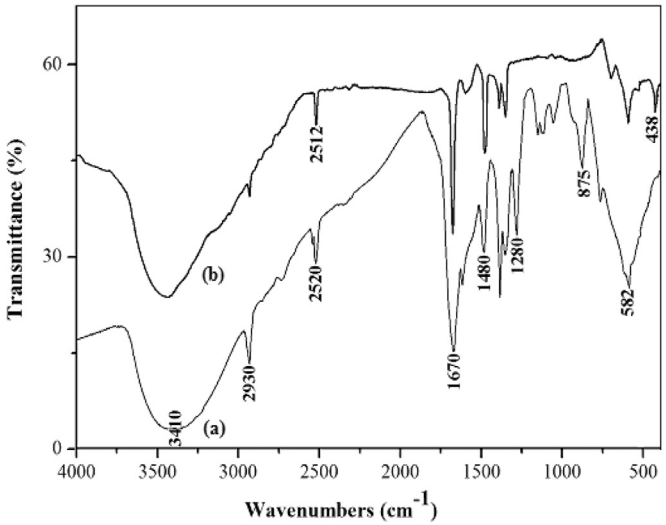

Fig. 1. FTIR spectra of 3 MPA capped Fe_3O_4 and after adsorption of Ni(II) on 3 MPA@MNPs.

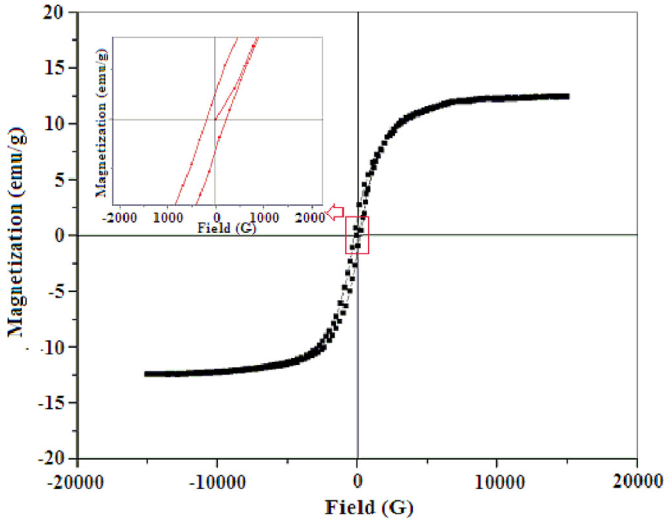

Fig. 3. Magnetization–hysteresis (*M–H*) loops of 3 MPA@Fe_3O_4 MNPs measured at room temperature. Upper inset shows the enlargement of the hysteresis loop at low magnetic field.

and 875 cm^{-1} are C–H stretching and free S–H stretching vibrations and CSH bending vibrations and also the characteristic band of Fe–O at 582 cm^{-1} was an indication of Fe_3O_4 MNPs [40]. In Fig. 1b the peak 2520 cm^{-1} shifted to 2512 cm^{-1} which assigned the changing of S–H stretching after adsorption and also a new peak at 438 cm^{-1} indicates the bonding between S–H and Ni(II) (Ni–S) bond [41]. The FT-IR technique, it was confirmed that the binding nature of COO^- and the presence of S–H on the surface of Fe_3O_4 nanocomposite and also coordination of S–H with Ni(II) metal ions.

3.2. TEM and EDS analysis

Fig. 2a represents the transmission electron microscopy (TEM) images of 3-mercaptopropanoic acid anchored Fe_3O_4 MNPs with scale 20 nm. The particles were nearly 11–18 nm size and also agglomerated because of 3-mercaptopropanoic acid ligand become interlinked on the surface of Fe_3O_4 MNPs through O–H and COO^- groups. This favors the stability of the colloidal dispersion. The spectrum was used to determine the elemental presence in the composition, which was revealed by EDS analysis. Fig. 2b shows the presence of sulfur in the sample with iron and oxygen. These results confirm the anchoring of 3-mercaptopropanoic acid on the surface of Fe_3O_4 MNPs.

3.3. Magnetic property

Fig. 3 shows the magnetic property of 3 MPA@Fe_3O_4 MNPs. Hysteresis loop of magnetic material showing the important parameters which are saturation magnetization (Ms) it demonstrates the complete magnetizability of magnetic materials, remanent magnetization(Mr). It reflects the magnetic field that is produced by the magnet after the magnetizing field has been removed and coercive force (Hc) characterizes the magnitude of the reverse field required to achieve demagnetization. The hysteresis loop demonstrates that the 3-mercaptopropanoic acid functionalized Fe_3O_4 MNPs have decreased ferromagnetic behavior when compared to pure Fe_3O_4 MNPs. The saturation magnetization (Ms), remaining magnetization (Mr), and coercive force (Hc) values were 14.02 emu/g, 1.43 emu/g and 191.77 G. An expanded hysteresis loops are shown in the inset (upper left) for field strengths between −1 k and 1 k to indicate hysteresis loop more clearly can

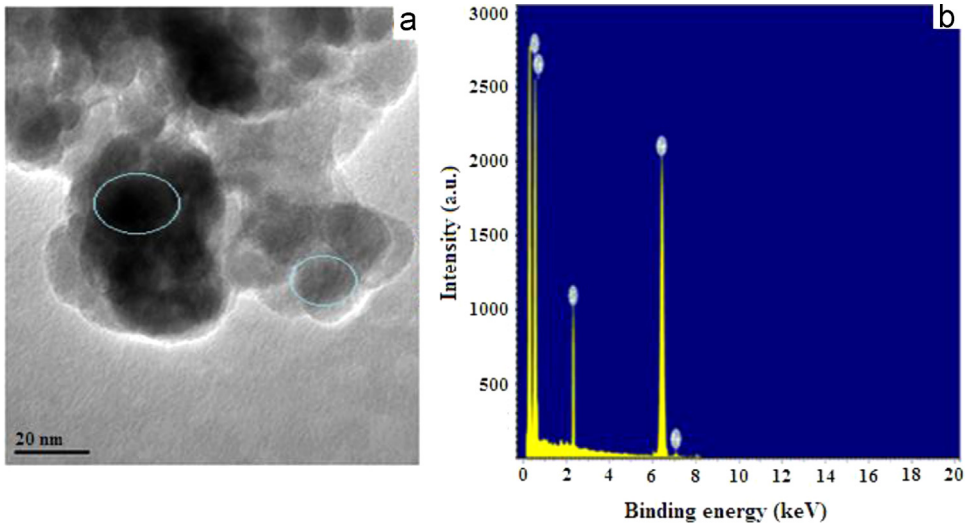

Fig. 2. TEM image of 3 MPA@Fe_3O_4 MNPs and EDS pattern of 3 MPA@Fe_3O_4 MNPs.

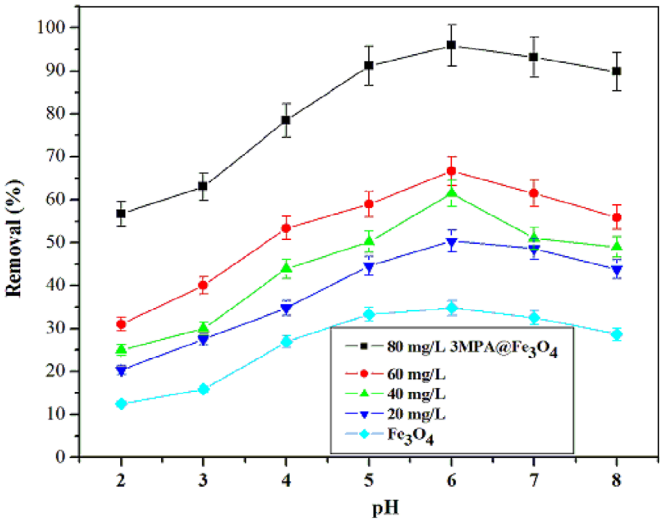

Fig. 4. Effect of pH value on the adsorption of Ni(II) by 3 MPA@Fe_3O_4 MNPs at different. Initial concentrations of Ni(II) (initial concentrations of Ni(II): 20, 40, 60, 80 mg/L, material dosage: 0.1 g/L, solution volume: 20 m/L, time: 120 min, temperature: 303 K).

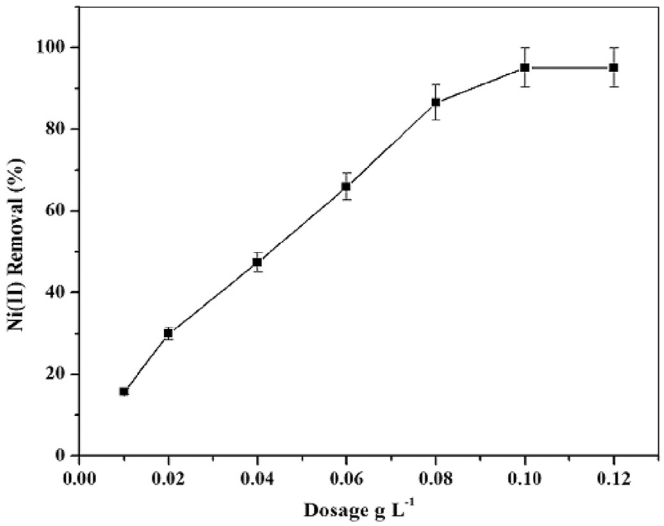

Fig. 5. Effect of adsorbent dosage on Ni(II) adsorption by 3 MPA@Fe_3O_4 MNPs.

see the nanoparticles contain ferromagnetic behavior. The results also show nonzero remnant magnetization (Mr) and coercive force (Hc) with non-linear hysteresis loop reveals ferromagnetic character [42]. The decrease of saturation magnetization of functionalized nanoparticles is due to the interaction between the coated 3 MPA and Fe_3O_4 may also quench the magnetic moment.

3.4. Effect of pH

The pH of solution is one of the most important variables, The effect of pH value on Ni(II) adsorption with 3 MPA@Fe_3O_4 nanoadsorbent was investigated at pH 2-8, 303 K and an different Ni(II) initial concentrations of 20, 40, 60 and 80 mg/L. As shown in Fig. 4 the percentage removal of Ni(II) increased with an increase of pH from 2 to 6 while decreased with a further increased pH. The nanocomposite displayed a maximum removal 95.90% at pH 6.0, an initial concentration of 80 mg/L. However, the removal efficiency was slightly Inhibited pH > 6 because of the formation of Ni (II) as $Ni(OH)_2$ [43].While the less affect was observed when the initial concentration of Ni(II) was as 20, 40 and 60 mg/L. The pH value of the solution can affect the surface charge of 3 MPA@Fe_3O_4 MNPs, which impact the adsorption of metal ions on the surface of the magnetic adsorbent. At lower pH Ni(II) removal was inhibited because of the H^+ competed with Ni(II) for adsorption sites, which significantly affected Ni(II) adsorption at low pH medium. Bare Fe_3O_4 (sky blue color) shows less than 40% removal efficiency, it clearly shows the presence of 3-Mercaptopropionic acid enhances the removal capacity.

3.5. Effect of adsorbent dosage

Removal of Ni(II) using 3 MPA@Fe_3O_4 MNPs with different dosages was investigated. The optimal adsorbent dosages varying from 0.01 to 0.12 g L^{-1} was shown in Fig. 5. The Ni(II) ion removal efficiency was gradually increased from 16 to ~96% as the dosage of 3 MPA@Fe_3O_4 MNPs increased from 0.01 to 0.1 g L^{-1}. The adsorption of Ni(II) increases, with increasing the adsorbent dose because more active sites on the adsorbent were obviously becoming available. However, it is saturated at 0.1 g L^{-1} dosage without showing further efficiency enhancement of Ni(II) ion removal. Thus, 0.1 g L^{-1} of 3 MPA@Fe_3O_4 MNPs was used in subsequent experiments.

3.6. Adsorption kinetic studies

The effect of contact time on the adsorption of Ni(II) ions by 3 MPA@Fe_3O_4 MNPs was studied. As shown in Fig. 6a the adsorption rate of the Ni(II) on adsorbent was almost finished within 60 min and reached equilibrium (initial concentration 80 mg/L, pH 6.0 at 303 K). The pseudo-first-order [44] and pseudo-second-order [45] kinetic models were used to investigate the kinetics of removal on the magnetic nanocomposite.

The linear form of pseudo-first-order kinetic model is described by the equation

$$\log(q_e - q_t) = \log q_e - \left(\frac{k_1}{2.303}\right)t \tag{3}$$

Where k_1 (min^{-1}) is the pseudo-first-order rate constant of adsorption, q_e (mg/g) and q_t (mg/g) are the amount of the Ni(II) adsorbed at equilibrium and at time t. The pseudo-first-order kinetic constant were determined from a slope of the plot of log ($q_e - q_t$) vs t. The R^2 value is very less (0.9045) suggesting that the adsorption of Ni(II) ions does not follow pseudo-first-order kinetic model.

The kinetic data was further analyzed using pseudo-second-order kinetic model. The linearized form of the equation is represented as

$$\frac{t}{q_t} = \frac{1}{k_2 q_e^2} + \left(\frac{1}{q_e}\right)t \tag{4}$$

Where k_2 (g/mg min^{-1}) is the pseudo-second-order rate constant, q_e (mg/g) and q_t (mg/g) are the amount of the Ni(II) adsorbed at equilibrium and at time t. The values of k_2 and q_e (0.0742 and 30.2839) can be calculated from the slope and intercept of a plot of t/q_t vs t. From the removal kinetics was shown in Fig. 6b the slope shows good linearity with the correlation coefficient value (R^2) which is 0.9914, as can be seen from the results, the correlation coefficients R^2 of pseudo-second order model (0.9914) were higher than that of pseudo-first-order model (R^2). Thus, the pseudo-second-order model fits better the experimental data than the pseudo-first-order model indicating the removal kinetic following the pseudo-second-order model. The corresponding parameters of the pseudo-second-order model were listed in Table 1. The adsorption system obeyed the pseudo-second-order kinetic

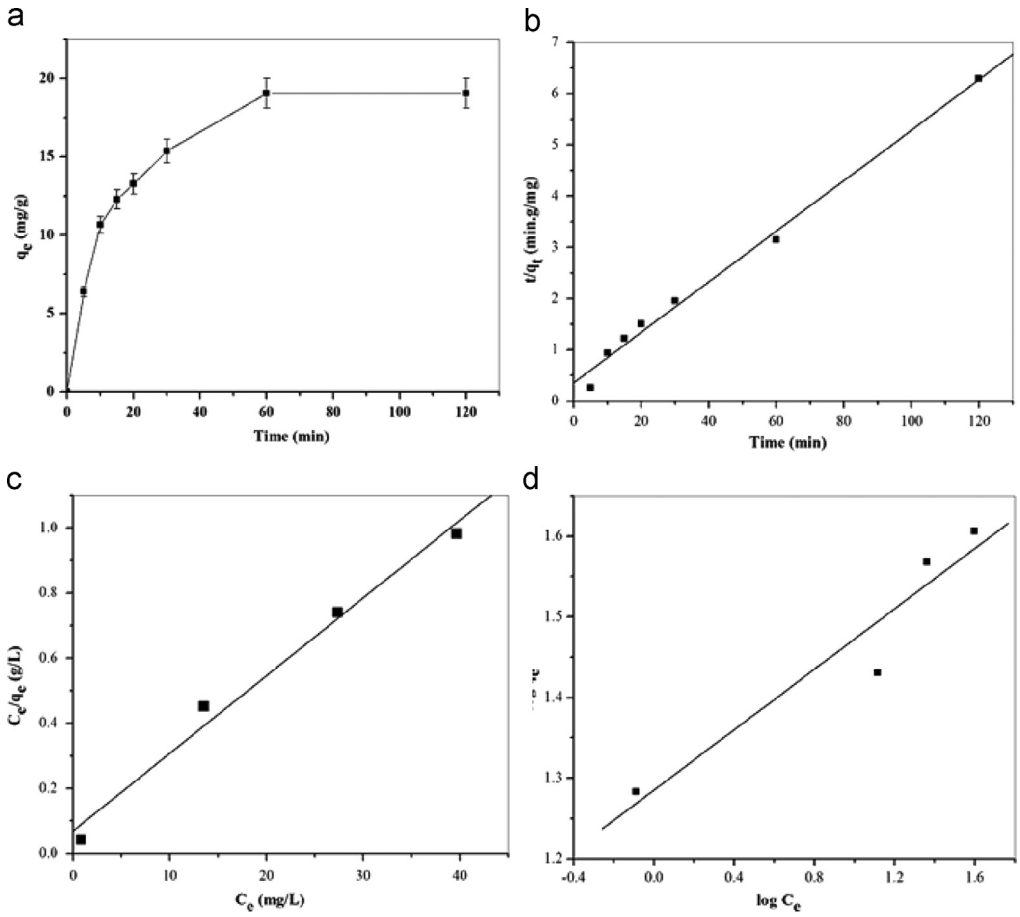

Fig. 6. (a) Effect of contact time on the extraction of Ni(II) by 3 MPA@Fe_3O_4 MNPs, (b). Pseudo second-order adsorption kinetics, (c) Linear plot of Langmuir isotherm and (d) Linear plot of Freundlich isotherm of Ni(II) on 3 MPA@Fe_3O_4 MNPs. and right inset shows the recycling efficiency.

model for the entire adsorption period and thus supported the assumption that the adsorption was the chemisorption process [46].

3.7. Adsorption isotherm

By using Langmuir and Freundlich isotherm models, the maximum adsorption capacity of adsorbent and the equilibrium adsorption of Ni(II) on 3 MPA@Fe_3O_4 MNPs was analyzed. The Langmuir equation can be expressed by the linearized form:

$$\frac{C_e}{q_e} = \frac{C_e}{q_m} + \frac{1}{q_m b} \tag{5}$$

where q_e is the equilibrium adsorption capacity of metal on concentration on the adsorbent (mg/g), C_e is the equilibrium metal ion concentration in the solution (mg/L), q_m is the maximum capacity of adsorbent (mg/g), and b (L/mg) is the equilibrium constant relating to the sorption energy. Fig. 6c shows that the experimental data fits the Langmuir adsorption isotherm well, maximum adsorption capacity was found to be 42.01 mg/g as prepared 3 MPA@Fe_3O_4 MNPs at pH=6.0 and correlation coefficients, equilibrium constants were listed in Table 2. In addition,

Table 1
Kinetic parameters of pseudo-second-order models for the adsorption of Ni(II) on the. MPA@Fe_3O_4 MNPs.

Pseudo-second-order			
$q_{e,}$ exp (mg/g)	k_2 (g/mg min^{-1})	$q_{e,}$ cal (mg/g)	R^2
29.0863	0.0742	30.2839	0.9914

another parameter in the Langmuir adsorption isotherm a dimensionless factor (R_L) is described by the following equation.

$$R_L = \frac{1}{1 + bC_i} \tag{6}$$

Where C_o (mg/g) is initial metal concentration, b (L/mg) is the Langmuir constant. For favorable sorption, $0 < R_L < 1$; for un favorable sorption, $R_L > 1$; for irreversible sorption $R_L < 0$; for linear sorption, $R_L = 1$. In this study, the R_L value is 0.0171 which lies between 0 to 1. This indicates that the adsorption of Ni(II) on 3 MPA@Fe_3O_4 MNPs is favorable.

The Freundlich isotherm can be applicable for modeling the adsorption of metal ions on heterogeneous surfaces and the linearized form of isotherm is expressed as

$$\log q_e = \log k_f + \frac{1}{n} \log C_e \tag{7}$$

where K_f (mg/g) and n are the Freundlich isotherm constants that represents the adsorption and the intensity of adsorbents, Fig. 6d shows the linear plot of Freundlich isotherm of Ni(II) adsorption on 3 MPA@Fe_3O_4 MNPs at 303 K. The fitted constants for the Freundlich isotherm model values of K_f, n and correlation coefficient (R^2) are calculated from the intercept and slope of the plot and are presented in Table 2. The values of $n > 1$ represent favorable adsorption condition [47,48] and the n value suggests that 5.3447 the 3 MPA@Fe_3O_4 MNPs is favorable for the adsorption of Ni(II) ions. Both the Langmuir and Freundlich isotherm models, Langmuir fit well with the adsorption data and have good correlation coefficients. Table 3. Shows the adsorption capacity of as prepared 3 MPA@Fe_3O_4 MNPs for Ni(II) from Langmuir isotherm

Table 2
Langmuir and Freundlich isotherm constants.

Isotherm	Parameters
Langmuir	
q_m (mg/g)	42.016
b (L/mg)	0.3429
R^2	0.9926
Freundlich	
k_f (mg/g)	19.288
n	5.3447
R^2	0.9570

Table 3
Comparison of adsorption capacities of Ni(II) on 3 MPA@Fe_3O_4 MNPs with other adsorbents.

Type of adsorbents	capacity (mg/g)	reference
Waste tea	15.26	[49]
Fe_3O_4 tea waste	38.30	[50]
Coir pith	9.50	[51]
Charcoal ash	10.86	[52]
Fe_3O_4/cyclodextrin polymer	13.2	[53]
Magnetic alginate microcapsules	30.5	[54]
MPA@Fe_3O_4 MNPs	42.01	This work

model compared with that of various adsorbents.

3.8. Effect of coexisting ions

Heavy metal pollutants are often present together with alkali and alkaline earth metal ions in water systems. It is necessary to study the selectivity of the adsorbent in the adsorption process. For this, 10 mg of adsorbent was added to 100 mL of aqueous solution containing different cations (Na^+, K^+, Mg^{2+},Ca^{2+} and Co^{2+}) with a concentration of 80 mg/L. The solution mixture was ultrasonication at room temperature for 5 min and transferred to 100 mL Erlenmeyer flask and was shaken in a thermostatic incubator (200 rpm) at 303 K. After that, the magnetic nano-adsorbent was removed magnetically from the solution. The data clarified that Ni(II) was readily absorbed by the adsorbent from multi-mixture ion solutions was shown in Fig. 7. The Ni(II) removal efficiency was more than 95%, indicating that the 3 MPA@Fe_3O_4 MNPs exhibited high selectivity to Ni(II)ions.

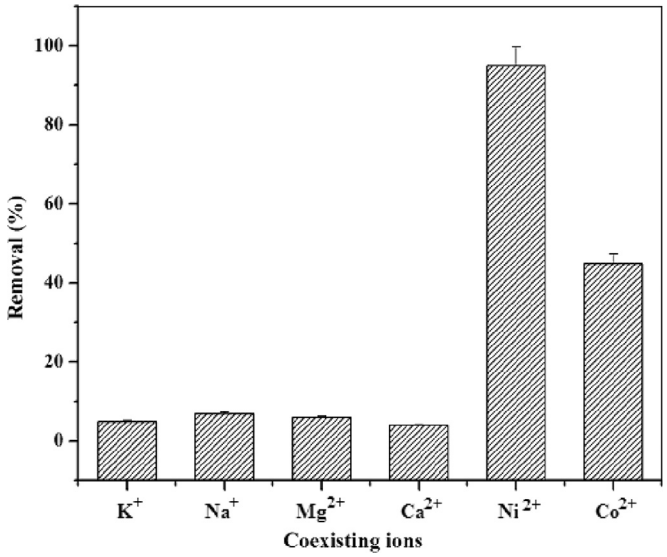

Fig. 7. selective removal of Ni(II) form mixed metal ion solution.

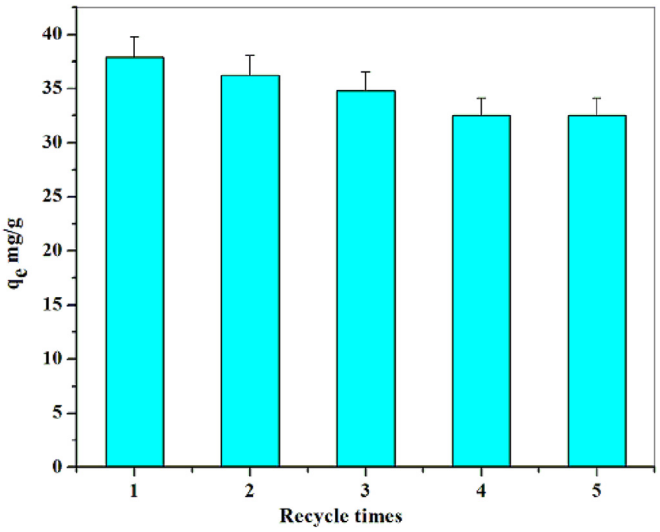

Fig. 8. Reusability of 3 MPA@Fe_3O_4 MNPs for five sequential cycles.

According to HSAB theory mercapto group have a strong bond with Ni(II) rather than other ions. This result clearly demonstrates selective adsorption of Ni(II) onto the surface of 3 MPA@Fe_3O_4 MNPs without interference from the other metal ions.

3.9. Desorption and reusability

It is essential the regeneration and reuse of an adsorbent. Owing to the environmental sustainability and economic efficiency. From the pH study, the adsorption percentage of Ni(II) is lower at lower pH value, acidic medium is expected to be a feasible approach for the regeneration of Ni(II) loaded 3 MPA@Fe_3O_4 MNPs. After adsorption, the desorption was carried out by washing out 3 MPA@Fe_3O_4 MNPs chelated Ni(II) with HCl (pH$\sim$2) and by rinsing adsorbent with double distilled water after that 3 MPA@Fe_3O_4 MNPs was dried at 90 °C and reused. It is observed that the adsorption capacity of Ni(II) slightly decreases from 37.9 to 36.2, 34.8, 32.5 and 32.5 mg/g and the recycling efficiency was higher than 75% after five cycles was shown in Fig. 8. Finally, the result shows us to believe that 3 MPA@Fe_3O_4 MNPs has great potential in decontamination of water from toxic metals.

4. Conclusions

To the best of our knowledge, this is the first report removal of Ni(II) by using biogenic 3 MPA@Fe_3O_4 MNPs. The 3 MPA@Fe_3O_4 MNPs can be used as an effective recyclable adsorbent for the removal of Ni(II) ions from aqueous solution. TEM, EDX, and FT-IR results indicate the surface characterization of 3 MPA@Fe_3O_4 MNPs. The strong electrostatic attraction present between Ni(II) and 3 MPA@Fe_3O_4 MNPs at various pH and plays a vital role in the adsorption mechanism. The maximum adsorption capacity was found to be 42.01 mg/g at pH 6, dose 0.1 g/L and temperature at 303 K. The pseudo-second-order kinetic model was fit rather than the pseudo-first-order kinetic model, This MNPs could achieve a rapid removal of Ni(II) from water with external magnet. These biogenic 3 MPA@Fe_3O_4 MNPs have promising application in the future environmental remediation process.

Acknowledgments

The author Sada Venkateswarlu thank to UGC-BSR, NewDelhi,

India No. F.7-187/2007(BSR), for providing financial support to carry out the present work. Also the authors thank to IIT-Madras and NEHU, Shillong for providing instrumental facilities.

References

[1] A. Celik, A. Demirba, Energy Sour. 27 (2005) 1167–1177.
[2] A. Ozer, G. Gurbuz, A. Calimli, B.K.J. Korbahti, J. Hazard. Mater. 152 (2008) 778–788.
[3] B.K. Reck, D.B. Müller, K. Rostkowski, T.E. Graedel, Environ. Sci. Technol. 42 (2008) 3394–3400.
[4] A.K. Shukla, S. Venugopalan, B. Hariprakash, J.Power Sour. 100 (2001) 125–148.
[5] K. Periyasamy, C. Namasivayam, Waste Manag. 15 (1995) 63–68.
[6] P. Katharina, K.R. Anna, B. Klove, Ecol. Eng. 75 (2015) 350–364.
[7] N. Akhtar, J. Iqbal, M. Iqbal, J. Hazard. Mater. B 108 (2004) 85–94.
[8] S.S. Arain, T.G. Kazi, J.B. Arain, H.I. Afridi, A.G. Kazi, S. Nasreen, K.D. Brahman, Environ. Sci. Pollut. Res. 21 (2014) 12017–12027.
[9] V. Coman, B. Robotin, P. Ilea, Resour. Conserv. Recycl. 73 (2013) 229–238.
[10] K. Kadirvelu, K. Thamaraiselvi, C. Namasivayam, Sep. Purif. Technol. 24 (2001) 497–505.
[11] L. Fang, W. Li, H. Chen, F. Xiao, L. Huang, P.E. Holm, H.C.B. Hansen, D. Wang, RSC Adv. 5 (2015) 18866–18874.
[12] Z. Liu, F.M. Doyle, Langmuir 25 (2009) 8927–8934.
[13] F. Fu, Q. Wang, J. Environ. Manag. 92 (2011) 407–418.
[14] I. Giannopoulou, D. Panias, Hydrometallurgy 90 (2008) 137–146.
[15] T. Subbaiah, S.C. Mallick, K.G. Mishra, K. Sanjay, R.P. Das, J. Power Source 112 (2002) 562–569.
[16] B. Alyuz, S. Veli, J. Hazard. Mater. 167 (2009) 482–488.
[17] I. Kabdasli, T. Arslan, T. Olmez-Hanci, I. Arslan-Alaton, O. Tünay, J. Hazard. Mater. 165 (2009) 838–845.
[18] S.A. Alaa, S.A. Amirah, J. Saud, Chem. Soc. 16 (2012) 451–459.
[19] M.A. Barakat, Arab. J. Chem. 4 (2011) 361–377.
[20] M. Kumari, B.D. Tripathi, Ecotoxicol. Environ. Safe 112 (2015) 80–86.
[21] P.J.L. Jones, J.R.R. Mendez, M. Streat, Process Saf. Environ. Prot. 82 (2004) 301–311.
[22] M. Kobya, E. Demirbas, E. Senturk, M. Ince, Bioresour. Technol. 96 (2005) 1518–1521.
[23] E. Ahmet, V. Nüket Tirtom, A. Tülin, B. Seda, D. Ayse, Chem. Eng. J. 210 (2012) 590–596.
[24] R.P. Srinivasa, Y. Vijaya, M.B. Veera, A. Krishnaiah, Bioresour. Technol. 100 (2009) 194–199.
[25] P. Panneerselvam, V. Sathya selva bala, N. Thinakaran, P. Baskaralingam, M. Palanichamy, S. Sivanesan, Eur. J. Chem. 6 (2009) 729–736.
[26] Y.F. Nava, M. Ulmanu, I. Anger, E. Maranon, L. Castrillon, Water Air Soil Pollut. 215 (2011) 239–249.
[27] S.S. Tahir, N. Rauf, J. Chem. Thermodyn. 35 (2003) 2003–2009.
[28] M. q Jiang, X. y Jin, X.Q. Lu, Z. l Chen, Desalination 252 (2010) 33–39.
[29] S. Yadav, V. Srivastava, S. Banerjee, C.H. Weng, Y.C. Sharma, CATENA100 (2013) 120–127.
[30] Y.C. Sharma, V. Uma, J. Srivastava, M. Srivastava, Chem. Eng. J. 127 (2007) 151–156.
[31] D.A. Ritu, S. Mika, Water purification using magnetic assistance: a review, J. Hazard. Mater. 180 (2010) 38–49.
[32] Y.C. Sharma, V. Srivastava, H. Weng, S.N. Upadhyay, Can. J. Chem. Eng. 87 (2009) 921–929.
[33] A.F. Ngomsik, A. Bee, M. Draye, G. Cote, V. Cabuil, C. R. Chim. 8 (2005) 963–970.
[34] K.G. Ravindra, G. Pavan, K.B. Sushmita, S. Shivani, K.S. Sanjeev, C.C. Mahesh, J. Mol. Liq. 204 (2015) 60–69.
[35] V. Srivastava, Y.C. Sharma, Water Air Soil Pollut. 225 (2014) 1–16.
[36] B.R. White, B.T. Stackhouse, J.A. Holcombe, J. Hazard. Mater. 161 (2009) 848–853.
[37] J.T. Mayo, C. Yavuz, S. Yean, et al., Sci. Technol. Adv. Mater. 8 (2007) 71–75.
[38] Y.C. Sharma, V. Srivastava, J. Chem. Eng. Data 55 (2010) 1441–1442.
[39] S. Venkateswarlu, B. NateshKumar, C.H. Prasad, P. Venkateswarlu, N.V. V. Jyothi, Physica B 449 (2014) 67–71.
[40] S. Venkateswarlu, Y. Subba Rao, T. Balaji, B. Prathima, N.V.V. Jyothi, Mater. Lett. 100 (2013) 241–244.
[41] P. Bharati, A. Bharti, M.K. Bharty, S. Kashyap, U.P. Singh, N.K. Singh, Polyhedron 63 (2013) 222–231.
[42] F. Mou, J. Guan, H. Ma, L. Xu, W. Shi, ACS Appl. Mater. Interfaces 4 (2012) 3987–3993.
[43] G.C. Panda, S.K. Das, T.S. Bandopadhyay, A.K. Guha, Colloids Surf. B: Biointerfaces 57 (2007) 135–142.
[44] Z.Y. Yao, J.H. Qi, L.H. Wang, J. Hazard. Mater. 174 (2010) 137–143.
[45] Y.S. Ho, G. Mckay, Ho, Y.S. Mckay, G., Pseudo-second order model for sorption processes, Process Biochem. 34 (1999) 451–465.
[46] G. Crini, H.N. Peindy, F. Gimbert, C. Robert, Sep. Purif. Technol. 53 (2007) 97–110.
[47] J. Gong, T. Liu, X. Wang, X. Hu, L. Zhang, Environ. Sci. Technol. 45 (2011) 6181–6187.
[48] B.H. Hameed, D.K. Mahmoud, A.L. Ahmad, J. Hazard. Mater. 158 (2008) 65–67.
[49] M. Emine, N. Yasar, J. Hazard. Mater. 12 (2005) 120–128.
[50] P. Panneerselvam, M. Norhashimah, A.T. Kah, J. Hazard. Mater. 186 (2011) 160–168.
[51] A. Ewecharoen, P. Thiravetyan, W. Nakbanpote, Chem. Eng. J. 137 (2008) 181–188.
[52] R. Katal, E. Hasani, M. Farnam, M.S. Baei, M.A. Ghayyem, J. Chem. Eng. Data 57 (2012) 374–383.
[53] Z.M.B. Abu, B.Z.S. Zayed, W.J.D. Tay, H. Kus, S.U. Mohammad, Carbohydr. Polym. 91 (2013) 322–332.
[54] A.F. Ngomsik, A. Bee, J.M. Siaugue, V. Cabuil, G. Cote, Water Res. 40 (2006) 1848–1856.